

Valorization of hops by-product for development of active poly(butylene succinate) film

Angela Borriello^a, Angela Marotta^b, Leandra Leto^c, Martina Cirlini^c, Benedetta Chiancone^c, Prospero Di Pierro^{a,d}, Veronica Ambrogio^{b,*}, Elena Torrieri^a

^a University of Naples Federico II, Dept. of Agricultural Sciences, Portici, Italy

^b University of Naples Federico II, Dept. of Chemical, Materials and Production Engineering (INSTM Consortium–UdR Naples), Naples, Italy

^c University of Parma, Dept. of Food and Drug, Parma, Italy

^d Centre for Food Innovation and Development in the Food Industry (CAISIAL), University of Naples Federico II, Portici, Italy

ARTICLE INFO

Keywords:

Hop by-product powder (HBP)
Polybutylene succinate (PBS)
Biodegradable packaging
Antioxidant film
Fiber size
Food simulants

ABSTRACT

Hop by-product powder (HBP), obtained from milling branches, leaves, and discarded cones, was valorized as a functional additive in polybutylene succinate (PBS) films to develop biodegradable antioxidant packaging. The HBP was first characterized for water absorption/desorption capacity and particle size distribution, then separated into three fractions based on fiber size (HBP-S: 63–160 μm; HBP-M: 160–220 μm; HBP-L: 220–710 μm). Total HBP (HBP-T) and each fraction were analysed for chemical composition and antioxidant properties. Four PBS composite films containing 10 wt.% of HBP-T, -S, -M, and -L were produced via melt blending, pelletizing, and compression molding. Their optical, thermal, mechanical, barrier, and water sorption properties were evaluated, together with antioxidant activity assessed by ethanolic extraction and in contact with food simulants. Smaller HBP particles exhibited higher cellulose content (≈79%), greater polyphenol concentration (≈10 mg GAE/g_{dw}), and stronger antioxidant activity (≈14 mg TEAC/g_{dw}). Incorporating HBP enhanced the films' elastic modulus and water absorption, shifting color toward red-yellow hues, particularly with smaller fibers. Fiber size had minimal impact on mechanical and thermal properties or antioxidant retention, suggesting that fractionation may be unnecessary. HBP maintained its antioxidant properties in PBS and demonstrated different release profiles in food simulants. The antioxidant activity of films increased over time, reaching values of 1.7 mg TEAC/g_{film} (DPPH, 7 days) and 23 mg TEAC/g_{film} (ABTS, 10 days). Simulants C and D1 had a higher capacity to solubilize antioxidant compounds from the film. These findings confirm HBP's potential to enhance PBS films functionality, making them promising for biodegradable antioxidant food packaging.

1. Introduction

The extraction of healthy substances from agrifood waste has increased in popularity recently, in line with the concepts of circular economy and sustainable technology (Panzella et al., 2020). Different agricultural waste, as fruit waste, shells, stalks and so on, have been introduced in a circular economy frame by reusing them for biogas production (Ning et al., 2021), antioxidant molecules extraction (Jimenez-Lopez et al., 2020), and active packaging production (Mohd Basri et al., 2021), showing specially a great potential as fillers in polymer-based composites (Marotta et al., 2025), offering both environmental and performance benefits.

Hop (*Humulus lupulus* L.), is traditionally cultivated for its cones,

primarily used in the brewing industry, generating a substantial amount of vegetative biomass of about 2.6 kg per plant, typically discarded or composted by growers (Abram et al., 2025; Sarraf et al., 2012). In recent years, increasing attention has been directed toward the valorization of this underutilized biomass, particularly hop leaves, which have been shown to be a rich source of bioactive compounds, comparable to the cones themselves (Chiancone et al., 2023; Leto et al., 2024; Macchioni et al., 2022; Sabbatini et al., 2024; Yeasmen and Orsat, 2023). These compounds, including flavonols, prenylflavonoids, and proanthocyanidins, are known for their antioxidant, antimicrobial, and estrogenic activities, as reported by Censi et al. (2021) and Santarelli et al. (2022). From a practical standpoint, comprehensive characterization of the entire hop plant's vegetative biomass, and not just the leaves, would be

* Corresponding author.

E-mail address: ambrogio@unina.it (V. Ambrogio).

<https://doi.org/10.1016/j.fufo.2026.100899>

Received 25 July 2025; Received in revised form 1 January 2026; Accepted 2 January 2026

Available online 3 January 2026

2666-8335/© 2026 The Authors. Published by Elsevier B.V. This is an open access article under the CC BY license (<http://creativecommons.org/licenses/by/4.0/>).

valuable for identifying potential commercial applications for what has traditionally been considered agricultural waste. Recent studies have demonstrated the use of a powder derived from hop vegetative biomass as an ingredient in the formulation of functional bread. This bread was enriched with characteristic hop bioactive compounds, including xanthohumol, lupulone, and volatile organic compounds such as β -myrcene and α -humulene, and exhibited an extended shelf life (Viola et al., 2025).

The use of active compounds from agri-food waste is of particular interest in the production of active packaging for food preservation (Bhargava et al., 2020; Duguma et al., 2023). By the combination of biopolymers and fillers until today considered as a waste, materials with an added value can be produced, perfectly fitting the circular economy requirements. As an example, De'Nobili et al. (2021) proposed sunflower hulls, a waste of oil industry, as filler in pectin-based films keeping its antioxidant activity. Furthermore, incorporating citrus fiber into starch-based composites significantly enhanced the functional properties of the materials, enabling a controlled release of polyphenols in both aqueous and lipid-rich food simulants (Zhang et al., 2025). Similarly, carrot fibers were added to pectin obtaining films with antioxidant properties (Idrovo Encalada et al., 2016). In this case a dependence of antioxidant properties on the particle size was highlighted. This work adds to those reporting the dependence of composites properties on filler size (Aniško et al., 2024; Versino & García, 2018; Zafar & Siddiqui, 2021).

Among the bioderived and biodegradable polymers, PBS (Aziman et al., 2021; Nuamduang et al., 2024; Mohamad et al., 2022) and its blends with other biopolymers such as PLA (Yang et al., 2019; Wongphan et al., 2023) and PBAT (Pothinuch et al., 2024; Pattaraudomchok et al., 2024) were proposed in several works as matrix for active packaging. Few papers deal with the incorporation of hop fibers into PBS: in 2010, Zou et al. (2010) added high amount of hop bines (the same used for beer production) to PP to obtain lightweight composites, tested mainly for their mechanical properties and Mirowski et al. (2021) added spent hop after extraction with supercritical CO₂, as filler in PVC, while more recently Rodriguez-Urbe et al. (2023) tried to improve composites mechanical properties by the addition of maleic anhydride grafted polybutylene succinate adipate (PBSA) to compatibilize hop and PBSA. Recently, Harder et al. (2023) proposed hop fibers from the whole plant as reinforcement for PBSA, studying the effect of different fiber size (0.25 mm, 1 mm, and 2 mm) on composites mechanical properties. Their results showed that the 1 mm fibers, due to their more uniform distribution, produced composites with tensile strength comparable to neat PBSA but substantially improved tensile and flexural stiffness and strength. Brewers' spent grain, spent hop and spent yeast, wastes of beer production, were upcycled as functional filler for polycaprolactone, capable of reducing the polymer oxidation temperature. (Hejna et al., 2024). Brewery by-products were also utilized to develop active films exhibiting effectiveness against both hydrophilic and lipophilic radicals in various food simulants (Santos et al., 2025).

To the best of our knowledge, no studies have investigated the use of hop cultivation residues for the development of active composites, despite hop extracts being commonly employed for their antioxidant properties. Furthermore, the use of vegetative biomass formed by branches, leaves, and discarded cones after hop harvesting was never proposed before.

In this study, the vegetative biomass of plants belonging to the hop cultivar, Cascade. Cascade is an aromatic hop variety selected in 1972, derived from an unknown American variety, Fuggle, and Serebrianka. It has become one of the hops most widely globally cultivated, several regions of Italy included (Santagostini et al., 2020). Renowned for its high yield and disease tolerance, Cascade is prized by the brewing industry for the floral and fruity aroma of its cones (Santagostini et al., 2020; Rodolfi et al., 2019).

The objective of this study was to assess the suitability of hop by-product powder (HBP) as a functional additive for developing

biodegradable antioxidant poly(butylene succinate) (PBS) films. To this end, the first part of the study focused on characterizing HBP in terms of water absorption/desorption capacity and particle size distribution. Furthermore, HBP was fractionated based on fiber size, and both the unfractionated HBP and its fractions were analyzed for chemical composition, total (poly)phenol content, and antioxidant activity. Subsequently, the influence of fiber size on composite PBS/HBP films containing 10 wt.% of HBP or its fractions was evaluated with respect to optical, thermal, mechanical, barrier, and water absorption/desorption properties. Finally, the antioxidant activity of the films was assessed using DPPH and ABTS assays after contact with ethanolic solutions and various food simulants.

2. Materials and methods

2.1. Materials

2.1.1. Production of HBP

The hop vegetative biomass was harvested at the end of the annual growth cycle, after cone harvesting, of hop plants, cv. Cascade, grown at 'Azienda Agricola Ludovico Lucchi', located in Campogalliano (Emilia-Romagna Region, Italy; 44°42'19.9" N, 10°50'26.1" E). The fresh hop biomass, including branches, leaves, and discarded cones, was dried at 35°C, using a low-temperature dryer (mod. PKT 2022, Packtin srl, 42122 Reggio Emilia, RE, Italy) to $6 \pm 0.5\%$ RH. The dry hop biomass was, then, milled through a hammer mill (mod. Rapide 200Z, Nuova Guseo S. r.l., 29010 Villanova sull'Arda, PC, Italy) and sieved using a 1000 μ m sieve to obtain hop biomass powder (HBP), which was packed in low density polyethylene bags and stored at room temperature.

2.2. HBP characterization

The HBP was characterized in terms of water absorption/desorption capacity and particle size distribution (PSD) (Supplementary data). The HBP was separated into different fractions based on the PSD curve (Fig. S1b). HBP was let pass through sieves with screen size (X) of 710, 220, 160 and 63 μ m. The obtained fibers fractions were classified as small (HBP-S, $63 < X < 160$, ≈ 32 wt.% of HBP), medium (HBP-M, $160 < X < 220$, ≈ 23 wt.% of HBP) and big (HBP-L, $220 < X < 710$, ≈ 37 wt.% of HBP). The sample not fractionated is defined as HBP-T. All samples were characterized in terms of chemical composition, total (poly)phenol content, and antioxidant activity (DPPH assay).

2.2.1. Analysis of chemical composition of HBP

The biochemical composition of the whole HBP-T and its relative sieved fractions (HBP-L, HBP-M, HBP-S) on a dry mass basis included crude protein, crude ash, total extractives and carbohydrates content. Crude protein content was determined according to Kjeldahl's method ($N \times 6.25$). Crude ash content was determined by burning sample at 550°C in a muffle furnace for 5 h. The total extractives content was determined as reported below. Carbohydrates were estimated by difference, subtracting the protein, total extractives and ash content to 100% on a weight percentage (w/w) dry basis. Moreover, samples were subjected to compositional characterization of structural carbohydrates (Hemicellulose, Lignin and Cellulose, respectively) by using the gravimetric method as reported by Ayeni et al. (2015) with small modifications. temperature for a few minutes and brought to constant weight in a convection oven at 105°C. The % (w/w) of the extractives content was evaluated as the difference in weight between the raw biomass and extractive-free biomass.

Hemicellulose: 1 g of dried extractive-free biomass was transferred into a 250 mL Erlenmeyer flask added 150 mL of NaOH 0.5 M and boiled for 3.5 h. After cooling, it was filtered under vacuum and washed until neutral pH and then the residue was dried to a constant weight at 105°C. The difference between the sample weight before and after this treatment is the hemicellulose content (%w/w) of dry biomass.

Lignin: 0.3 g of dried extractive-free biomass was weighed in glass test tubes and 3 mL of 72% sulfuric acid was added. The sample was kept at room temperature for 2 h with carefully shaking at 30 min intervals to allow for complete hydrolysis. After that, the sample was transferred into glass bottle to obtain 4% final sulfuric acid with distilled water and subjected to the second step of hydrolysis in autoclave for 1 h at 121 °C. The slurry was then cooled at room temperature and filtered by using a Gooch crucible filter (G3) under vacuum. The acid insoluble lignin was determined by drying to constant weight at 105 °C the Gooch crucible filter subtracted the ash by incinerating the hydrolyzed samples at 575 °C in a muffle furnace and protein content according to Kjeldahl's method ($N \times 6.25$). The acid soluble lignin fraction was determined by measuring the absorbance of the acid hydrolyzed samples at 320 nm ($\epsilon=30$). The lignin content was calculated as the sum of acid insoluble lignin and acid soluble lignin.

Cellulose: The cellulose content (w% on dry basis) was calculated by difference subtracting to 100, hemicellulose, lignin, ash and protein (w% on dry basis).

2.2.2. Determination of total polyphenol content and antioxidant activity of HBP

Ethanol/water (80/20 v/v), with a dilution factor of 1:20, was used for performing the sample extraction.

Suspensions were placed in a shaker for 2 h, 200 strokes/minute, at room temperature on a digital agitator (HS 501, IKA-Werke GmbH & Co, Staufen, Germany (Carbone et al., 2020; Martelli et al., 2020)). To separate the extract from the solid fraction, a centrifuge (Centrifuge 4206, Alc International, Pévy, France) was used at 5000 rpm for 10 min, at room temperature. Each extraction procedure was repeated twice.

Total Polyphenols Content (TPC) and Antioxidant Activity (AO) of the samples were determined through different spectrophotometric assays, according to the protocol described by Chiancone et al. (2023). The TPC was determined through the Folin-Ciocalteu test while AO was evaluated by 2,2-diphenyl-1-picrylhydrazyl (DPPH) assay.

The spectrophotometer JASCO V-530 (Easton, MD, USA) has been used for sample evaluations; for the calibration curve of TPC five points were used into a range of 10-100 mg/kg of gallic acid and the results reported in mg/g GAE (Gallic Acid Equivalents). The same process was used for AO determinations, but the curve was constructed using 6-hydroxy-2,5,7,8-tetramethylchroman-2-carboxylic acid (Trolox) as standard and the results expressed in mg/g TEAC (Trolox Equivalent Antioxidant Capacity). Instrument has been set with feature absorbance at 760 nm for the TPC and 517 nm for DPPH (Chiancone et al. 2023).

A drying process was required to use the HBP for film production (Section 2.3). Thus, the TPC and AO were analyzed before and after the thermal treatment.

2.3. Preparation of PBS/HBP composites film

Polybutylene succinate (PBS), a food grade bioderived, biodegradable and compostable polymer, was selected as matrix to produce hop-filled composites. BioPBS™ FZ71PM was supplied by Mitsubishi Chemical Corporation. PBS and 10 wt.% of each HBP fraction (HBP-T, HBP-S, HBP-M and HBP-L) were melt-blended using a Process11 (ThermoScientific) twin-screw extruder, at 180 °C and 80 rpm. Prior to processing both PBS and hop fibers were dried overnight in a vacuum oven at 80 °C. The recovered melt was pelletized and then compression-molded into thin sheets, by using a P300P Collin hydraulic press at 140 °C and 0.5 bar. The obtained films were named PBS/HBP-T, PBS/HBP-S, PBS/HBP-M, PBS/HBP-L.

2.4. Characterization of PBS/HBP composites film

PBS/HBP composites film were characterized in terms of physical and antioxidant properties. Optical, thermal, mechanical, barrier, water adsorption/desorption and antioxidant properties were investigated as

follows.

2.4.1. Optical properties

The color parameters of the films were determined using a colorimeter (CR-400, Minolta, Osaka, Japan). The obtained values corresponded to L^* (lightness), a^* (red–green coordinate), and b^* (yellow–blue coordinate). The total color difference (ΔE) between neat PBS and PBS/HBP composites films, and chroma (C) were calculated according to Eqs. (1) and (2), respectively (Mizielnińska et al., 2024):

$$\Delta E = \sqrt{(\Delta L)^2 + (\Delta a)^2 + (\Delta b)^2} \quad (1)$$

$$c^* = \sqrt{(a^*)^2 + (b^*)^2} \quad (2)$$

Opacity was measured at 660 nm using a spectrophotometer (JASCO V550, Tokyo, Japan) and reported as absorbance per film thickness (mm). Thickness was assessed with a digital micrometer (H062, Meta-control, Naples, Italy; resolution $\pm 2 \mu\text{m}$), following the procedure described by Borriello et al. (2025).

2.4.2. Thermal and morphological properties of PBS/HBP composites film

Thermogravimetric analyses (TGA) were performed with a TA Q500 under nitrogen flux, heating samples from 40 to 700 °C at a 10 °C min⁻¹ heating rate. The temperature at which the degradation process is faster (T_{dmax}) is evaluated as the maximum of the TGA derivative.

Crystallinity and thermal stability of the PBS/HBP films were determined by calorimetric techniques. Differential scanning calorimetry (DSC) tests were conducted with a TA Q20 equipped with RSC90 cooler, heating samples from -50 °C to 200 °C with 10 °C min⁻¹ heating rate under a nitrogen flux of 50 mL min⁻¹. After the first heating scan, the sample was cooled at the same heating rate to -50 °C and then heated again up to 200 °C. Samples crystallinity (χ) was evaluated, for each heating scan, by Eq. (3),

$$\chi = \frac{\Delta H_m - \Delta H_{cc}}{(1 - \phi) \Delta H_{100}} \cdot 100\% \quad (3)$$

where ΔH_m is the enthalpy of melting, ΔH_{cc} is the enthalpy of cold crystallization, ϕ is the mass fraction of the filler (i.e. 0.1) when present, and ΔH_{100} is the enthalpy of fusion of fully crystalline PBS, which is 110.3 J g⁻¹ (Ou-Yang et al., 2018). From DSC thermograms the glass transition temperature (T_g) of the PBS/HBP films was evaluated.

Different parameters of DSC and TGA were estimated by TA Instrument TRIOS Software (Version 5.1.1.46572).

X-ray diffraction (XRD) analyses were performed using a X'Pert Pro (PANalytical) diffractometer with a Cu K α radiation. The 2 θ range analyzed was 5–60° with step size of 0.013° in 2 θ and scan speed of 0.04° 2 θ /s. Samples crystallinity (χ_c) was evaluated as the ratio between the area of crystalline peaks (A_c) and the sum of crystalline and amorphous areas (A_a), as reported in Eq. (4)

$$\chi_c = \frac{A_c}{A_c + A_a} \cdot 100\% \quad (4)$$

2.4.3. Mechanical properties of PBS/HBP composites film

Mechanical properties were evaluated by tensile tests, following ASTM D638 and UNI EN ISO 527 tests. PBS/hop composite films of ~200 μm thickness were cut into strips of about 13 mm width and 150mm length. Tensile tests were conducted at a crosshead speed of 10mm/min with a Tensometer 2020 on 5 replicates for each sample. From the recorded stress-strain curves the elastic modulus (E), maximum stress (σ_{max}), and maximum elongation (ϵ_{max}) values were extrapolated.

2.4.4. Oxygen barrier properties of PBS/HBP composites film

The barrier properties of the films were evaluated using a Totalperm permeability tester (ExtraSolution, Italy), designed for the

determination of gas transmission rates through thin film. Oxygen permeability (P) was measured according to ASTM D3985, using high-purity oxygen as the test gas and nitrogen as the carrier gas. Tests were carried out at 25°C, and the oxygen transmission rate (OTR) values were automatically recorded by the instrument and normalized to film thickness.

2.4.5. Water adsorption/desorption isotherm of PBS/HBP composites film

The adsorption and desorption isotherms of the total HBP were measured at 30°C following the procedure described by Borriello et al. (2025), with some adjustments. The analysis was performed using a microbalance system (DVS dynamic vapor sorption Q500SA, TA Instrument, New Castle, USA) capable of measuring with 0.1 mg precision. Samples of PBS and PBS/HBP composite films (5 mg) were first stabilized at 0% relative humidity (RH) until their weight remained stable. Relative humidity was then incrementally increased from 10% to 90% to assess adsorption and subsequently decreased from 90% back to 10% to evaluate desorption. At each humidity step, samples were held until the weight variation was below 0.001% for 10 min. The resulting isotherms were plotted as equilibrium moisture content versus water activity (a_w).

2.4.6. Antioxidant activity of PBS/HBP composites film

The antioxidant activity of the PBS/HBP composite film was assessed by measuring the scavenging activity of compounds extracted from the film against the DPPH•+ and ABTS•+ radicals. Extracts were obtained after exposing the film to i) an ethanolic solution and ii) different food simulants: i) a 6 cm² section of each film sample was immersed in 10 mL of an ethanol/water mixture (80:20 v/v) and left until equilibrium was reached; ii) four different food simulants were selected based on European Commission Regulation (EU) from October 2011: A (10% ethanol v/v), B (3% acetic acid w/v), C (20% ethanol v/v), and D1 (50% ethanol v/v). For each simulant, 3 cm² of film was submerged in 5 mL of solution and stored at 40°C for 1, 3, 7, and 10 days. DPPH•+ (2,2-diphenyl-1-picrylhydrazyl) assay was performed according to Khan et al. (2022) with modifications. In brief, 1 mL of supernatant was added to 1.5 mL of DPPH working solution (25 ppm) and kept in the dark for 30 min at 25°C. Absorbance readings were taken at 517 nm using a UV-VIS spectrophotometer (JASCO, V550, Tokyo, Japan). The percentage of DPPH radical scavenging was determined using Eq. (5):

$$DPPH (\%) inhibition = \frac{A_C - A_F}{A_C} \cdot 100 \quad (5)$$

where A_C is the absorbance of the control and A_F is the absorbance of the film.

For the ABTS•+ (2,2'-azinobis-3-ethyl-benzothiazoline-6-sulfonic) assay, the procedure was adapted from Hanani et al. (2019). A volume of 100 µL of food simulants was combined with 1 mL of ABTS solution (7 mM). The absorbance was measured at 734 nm after 3 min of incubation against a negative control (1 mL of ABTS solution and 100 µL of distilled water). The results are expressed as mg Trolox equivalent antioxidant capacity (TEAC)/g film.

2.5. Data analysis

Results are presented as the mean ± standard error of at least three replications. The widely accepted Guggenheim-Anderson-de Boer (GAB) model (Eq. (6)) was adopted to fit experimental data of water adsorption isotherms. The equation was reformulated as follows:

$$X = \frac{m_0 \times C \times a_w}{(1 - K \times a_w) \times (1 - K \times a_w + C \times K \times a_w)} \quad (6)$$

where m_0 is the moisture content of the monolayer ($g_{water} g_{dry\ film}^{-1}$), K and C are dimensionless constants of the model, and a_w is the water activity. To measure the accuracy of the GAB models, the root-mean-square error (RMSE) (Eq. (7)) was used:

$$RMSE = \sqrt{\frac{\sum (Ve - Vp)^2}{n}} \quad (7)$$

where Ve and Vp correspond to the experimentally measured and model-predicted values, respectively, and n is the total number of observations.

Two-way Analysis of Variance (ANOVA) (Tukey's test, $p < 0.05$) was performed to evaluate whether differences among HBP total (poly) phenol content and antioxidant activity (DPPH), due to the factors "Particle size" and "Thermal treatment", were statistically significant. When only one factor was significant, one-way ANOVA was performed. Statistical analysis was performed by using SYSTAT 13.1 (Systat Software, Inc; Pint Richmond, CA). To determine significant differences among PBS/HBP composite films based on HBP fiber size, one-way ANOVA followed by Duncan's multiple range test ($p \leq 0.05$) was applied. Additionally, variations in antioxidant activity caused by different contact times and types of food simulants were also assessed using the same approach. Statistical analyses were conducted using SPSS software (version 17.0, SPSS Inc., Chicago, IL, USA).

3. Results and discussion

3.1. Chemical composition of HBP

The biochemical composition of HBP-T is characterized by: 10.19 ± 0.03% ash, 14.76 ± 0.34% proteins, 10.10 ± 0.23 % extractives and 64.55 ± 0.64% carbohydrates. These results confirm the higher content of polysaccharides that is characteristic of vegetable tissue, mainly represented by fiber. To understand the distribution of various fiber types within HBP-T and its sieved fractions (HBP-L, HBP-M, and HBP-S), we characterized the samples for polysaccharide composition (cellulose, hemicellulose, and lignin). As shown in Table 1, compositional variations were observed across the fractions. Lignin and hemicellulose content decreased with decreasing particle size, while cellulose and extractives (including polyphenols, bitter acids, and essential oils) increased. This is likely due to the inherent heterogeneity of the starting biomass (branches, leaves, and cones) and the differential grinding behavior of fibrous and non-fibrous tissues. It is well-established that these tissue types respond differently to grinding, resulting in varying particle sizes. Fibrous tissues, such as hop bines, are composed of long, strong fibers that provide structural support. While grinding breaks these fibers, they retain some length and strength, yielding a coarser texture with larger particles. These fibrous tissues are distributed throughout the hop plant and are rich in lignin, hemicellulose, and cellulose. In contrast, non-fibrous tissues, such as leaves and cones, are softer and more delicate. Grinding these tissues results in smaller, more

Table 1

Chemical composition of HBP and relative sieved fractions (HBP-L, HBP-M, and HBP-S).

Composition(% dw)	Sample (µm)			
	HBP-T	HBP-L (220<X<710)	HBP-M (160<X<220)	HBP-S (63<X<160)
Proteins	14.76 ±0.34	13.24±2.33	9.25±2.55	21.32±3.37
Total extractives	10.10 ±0.23	2.21±2.71	5.17±2.49	8.60±4.88
Ash	10.19 ±0.03	8.62±1.47	5.23±1.18	8.40±0.41
Carbohydrates	64.55 ±0.64	75.93±3.21	80.35±2.01	61.70±1.17
Hemicellulose (%)	40.50 ±1.42	44.42±0.20	33.82±3.08	14.61±5.75
Lignin (%)	12.20 ±1.11	16.10±3.42	13.11±1.93	6.56±2.28
Cellulose (%)	47.3 ±2.13	39.48±0.91	53.07±2.52	78.83±8.35

uniform particles due to their less rigid structure. These tissues, primarily composed of epidermis and mesophyll-like tissue, are characteristically rich in cells involved in photosynthesis, storage, and secretion. Cellulose, the primary structural component of plant cell walls, is present in both types of tissue, though its relative concentration increases in smaller particle fractions.

3.2. Total (Poly)Phenol Content and Antioxidant Activity of HBP

The HBP-T presented a TPC of 9.13 ± 0.18 mg GAE/g (dry weight) and an AO of 13.58 ± 2.07 mg TEAC/g (dry weight).

An increase in polyphenol content, and consequently in molecules with antioxidant activity in plant matrices, depends on several factors such as solvents, temperature, and extraction time. In this context, several scientific studies have demonstrated that temperature treatment of plant biomass reduces water content and leads to a higher concentration of biomolecules (Durling et al., 2007; Antony and Farid, 2022; Netshiluvhi and Eloff, 2024). The statistical analysis carried out on fractionated HBP, before and after the drying process, highlighted that the parameter TPC was influenced exclusively by the factor “Particle size” (Table 2); specifically, as the particle size increased, the TPC significantly decreased. The same trend was observed for AO response of the different particle size of HBP; in fact, as observed for TPC, statistical analysis evidenced that there is a significant decreasing in AO from HBP-S to HBP-L. Moreover, if the thermal treatment does not seem to have affected the TPC of HBP, it has influenced the AO, independently of the sample particle size. In fact, statistical analysis evidenced that AO increased significantly after the thermal treatment.

3.3. Physical properties of PBS/HBP composites film

The HBP inclusion into a polymeric matrix, preferably bioderived and biodegradable helps handling fibers to easily benefit their properties. For this reason, the different HBP fractions (i.e. HBP-T, HBP-S, HBP-M, and HBP-L), were incorporated into PBS through a melt mixing process and formed to obtain films. These films were characterized in terms of optical, thermal, mechanical, barrier and water adsorption/desorption properties.

The colour parameters and opacity of PBS and PBS/HBP composites film are reported in Table 3, while their visual appearance is shown in Fig. 1. PBS films typically exhibit a milky and opaque appearance, consistent with observations reported in previous studies (Łopusiewicz et al., 2021; Macieja et al., 2025). The lightness (L^*) of the films decreased markedly with the incorporation of HBP, dropping from 91.69 ± 0.14 for neat PBS to 57.02 ± 0.01 for PBS/HBP-S, indicating a significantly darker appearance ($p < 0.05$). The incorporation of HBP led to a significant increase in both redness (a^*) and yellowness (b^*), with

Table 2

Influence of particle size and thermal treatment on total (poly)phenol content (TPC) and antioxidant activity (AO) of the powder, derived from hop vegetative biomass.

Particle size	Thermal treatment	TPC (mg GAE/g _{dw})	±DS	DPPH (mg TEAC/g _{dw})	±DS
63-160 μm (HBP-S)	NTT	10.58	0.71	13.33	1.17
	TT	10.83	0.38	14.45	0.51
160-220 μm (HBP-M)	NTT	7.71	0.36	10.71	0.86
	TT	8.34	0.68	11.36	0.58
220-710 μm (HBP-L)	NTT	5.60	0.59	7.43	0.37
	TT	5.90	0.41	8.13	0.43
Statistical analysis		p		p	
Particle size (PS)		0.000		0.000	
Thermal treatment (TT)		0.093		0.010	
PSxTT		0.752		0.769	

Two-way ANOVA, Tukey's test $p < 0.05$. NTT: Non thermal treated hop by-product powder (HBP); TT: HBP treated at 80°C overnight.

Table 3

Optical properties of films: color (L^* , a^* , b^*), total color difference (ΔE), chroma (C), and opacity of films.

	L^*	a	b	ΔE	C	Opacity (A mm ⁻¹)
PBS	91.69 ±0.14 ^c	-0.33 ±0.04 ^a	4.93 ±0.14 ^a	0.00 ±2.19 ^a	4.94 ±0.13 ^a	4.57 ±0.11 ^a
PBS/ HBP- T	64.35 ±2.15 ^b	5.55 ±0.45 ^b	29.52 ±0.91 ^b	37.27 ±2.19 ^a	30.04 ±0.93 ^b	7.81 ±0.26 ^b
PBS/ HBP- L	67.43 ±0.81 ^b	5.97 ±0.16 ^b	29.29 ±0.21 ^b	34.96 ±0.71 ^a	29.89 ±0.21 ^b	8.06 ±0.35 ^b
PBS/ HBP- M	57.28 ±0.40 ^a	8.31 ±0.07 ^c	31.03 ±0.20 ^c	44.05 ±0.30 ^b	32.12 ±0.19 ^c	8.07 ±0.08 ^b
PBS/ HBP- S	57.02 ±0.01 ^a	8.21 ±0.00 ^c	30.65 ±0.02 ^c	44.80 ±0.45 ^b	31.73 ±0.01 ^c	8.04 ±0.01 ^b

the most pronounced color shifts observed in films containing M- and S-sized fibers. The total color difference (ΔE) between neat PBS and PBS/HBP composites films exceeded 1.00, a threshold generally regarded as perceptible to the human eye (Łopusiewicz et al., 2021). ΔE values ranged from 34.96 ± 0.71 (PBS/HBP-L) to 44.8 ± 0.45 (PBS/HBP-S) which are considerably higher than those reported in the literature for PBS-based films enriched with quercetin (Łopusiewicz et al., 2021). The incorporation of HBP markedly increased the chroma (C^*) values, indicating a higher color saturation of the films and reflecting a more intense and vivid coloration compared to the neat PBS matrix. The opacity of the films increased significantly with the incorporation of HBP, primarily due to the presence of phenolic compounds and lignin (Qin et al., 2025). This enhancement in opacity, as well as in darkness, may render the PBS/HBP composite films effective barriers against light-induced oxidation, preserving nutrients, color, and flavor in food applications.

By the thermal characterization of PBS/HBP films it emerges that the addition of HBP does not affect the thermal resistance of composites, regardless of the fraction embedded in PBS, as highlighted by TGA analysis, reported in Fig. 2a. PBS/HBP composites film preserves the high thermal resistance of PBS, whose degradation temperature is close to 400°C (Table 4). The effect of HBP incorporation on thermal properties can be noticed in the appearance of a shoulder in the DTG curve below 300°C and from the small weight loss observed around 100°C. The main degradation processes of HBP occur between 200°C and 300°C; therefore, the presence of HBP fibers results in a slight initial degradation step in all composites within this temperature range. In addition, HBP-T is hydrophilic and can absorb significant amounts of water (~10 wt.%), which evaporates during the TGA analysis at around 100°C, even when the fibers are embedded in PBS. After the main degradation stage, all samples exhibit a final residue corresponding to a carbonaceous char. The residue measured for the composite samples is consistent with the amount of incorporated fibers, considering the contributions from both PBS and HBP.

In Fig. 2b, the DSC thermograms of heating and cooling scans for PBS and PBS/HBP films are reported, and in Table 5 the main thermal parameters derived are summarized. The addition of HBP-S, HBP-M, and HBP-L fibers fractions, as well as HBP-T fibers have no effect on the glass transition temperature of composites and on their crystallinity. The crystallinity recorded during the first heating scan (χ_1 , Table 5) is related to the samples' thermal history imposed during the production process while χ_2 , evaluated on the melting enthalpy recorded during the second heating scan, is only affected by the particle-matrix interactions. The results of thermal analysis on PBS/HBP films reveal a not significant nucleating effect of fibers, as also reported for different fillers in PBS (Li et al., 2015), as well as for other semicrystalline polymers filled with

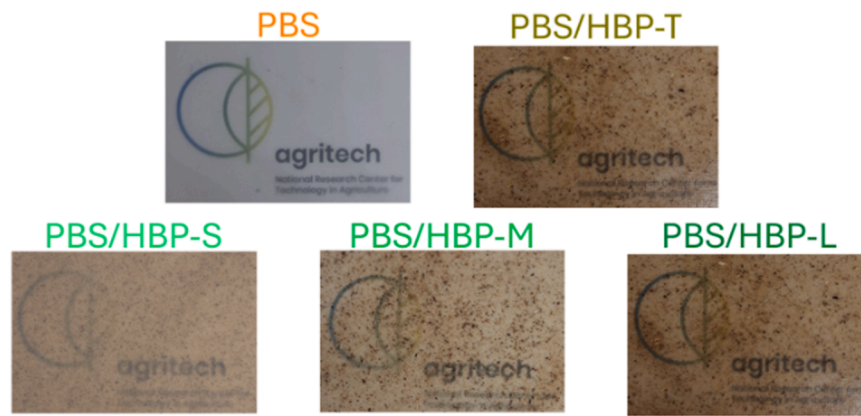


Fig. 1. The visual appearance of neat PBS and PBS/HBP composite films.

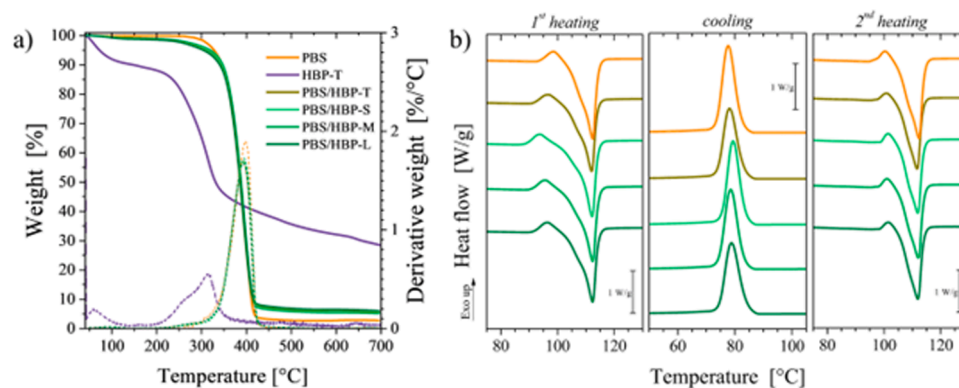


Fig. 2. Thermal properties of films. a) TGA and b) DSC thermograms of PBS, HBP-T and PBS/HBP composite film.

Table 4

Temperature at 5 % weight loss (T_{d5}), temperature at maximum degradation rate (T_{dmax}) and weight residue at 700 °C for PBS, HBP-T and PBS/HBP composites film.

	T_{d5} [°C]	T_{dmax} [°C]	R_{700} [%]
PBS	328.1	398.8	2.76
HBP-T	72.3	313.6	28.41
PBS/HBP-T	309.3	392.0	5.84
PBS/HBP-S	315.4	397.4	5.18
PBS/HBP-M	319.4	395.4	5.16
PBS/HBP-L	304.4	393.7	6.03

natural fibers (Barczewski et al., 2023). The samples crystallinity was further evaluated by XRD analysis (Table 5), confirming what was gathered by DSC analysis. The values of χ_c is not significantly affected by the HBP incorporation. Furthermore, the XRD diffractograms of PBS show the typical diffraction peaks at 2θ of 19.6° and 22.6°, corresponding to the (020) and (110) planes, respectively, and a peak at about 22° (visible as a shoulder of the main peak) corresponding to the (110) plane (Fig. S3) (Xu et al., 2022). Upon fiber addition, no significant peak shifts were observed, indicating that no new crystalline phase was formed.

Tensile tests on PBS/HBP composite films were performed to evaluate the impact of fibers addition to the polymer in terms of mechanical properties (Fig. 3). As can be expected, the addition of fibers induces an increase in the elastic modulus, as was also proven by Harder et al. (2023), but half the ultimate strength and the elongation at break of the material. As generally reported in the literature, the sample containing the fibers fraction with the highest content of cellulose (i.e. the HBP-S fraction) has the best tensile strength compared to other fractions

(Ortega et al., 2022), and the best elongation at break, likely due to the finer dispersion of the smaller fibers within the matrix (Makri et al., 2022). Nevertheless, HBP is a fine powder made by small fibers (i.e., fiber length < 1 cm) so no reinforcement effect was expected, but the addition of this kind of active filler can impart antioxidant properties to PBS.

The oxygen permeability of the films was also evaluated, and the results are reported in Table 5. The addition of fibers to PBS adversely affects the barrier properties, particularly as the fiber dimensions increase. In this case, the fiber size (see Supporting Information) is comparable to or even larger than the film thickness. As a consequence, the fibers may act as preferential pathways for oxygen diffusion through the film. Conversely, in the PBS/HBP-S system, the filler size is smaller than the film thickness, and the permeability shows only a slight increase, probably due to an enhanced free volume within the polymer matrix arising from the fiber–matrix interfaces, also responsible of the decrease

Table 5

Glass transition temperature (T_g), crystallinity measured by DSC (χ_1 , χ_2) and by XRD (χ_c) and permeability (P) for PBS and PBS/HBP composites film.

	T_g [°C]	χ_1 [%]	χ_2 [%]	χ_c [%]	P [cm ³ (STP) cm/(m ² 24h atm)]
PBS	36.7	50.8	51.3	54.7	0.72
PBS/HBP-T	34.3	48.9	49.6	53.6	4.86
PBS/HBP-S	36.7	52.2	51.0	52.7	2.40
PBS/HBP-M	36.8	53.9	52.1	52.9	28.22
PBS/HBP-L	36.9	50.5	50.7	53.2	45.52

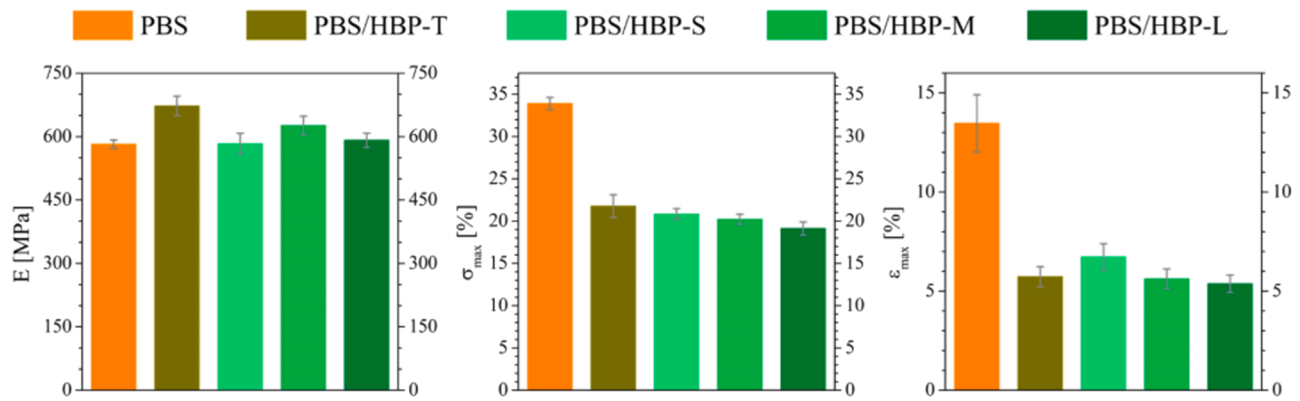


Fig. 3. Mechanical properties of films. Values of elastic modulus (E), ultimate strength (σ_{max}) and deformation at break (ϵ_{max}) for the PBS/HBP composites film.

of composites' mechanical properties.

The moisture adsorption and desorption isotherms of the PBS and PBS/HBP composites film are reported in Fig. 4(a,b). The isotherms showed a sigmoidal-shaped profile and two bending regions, one around 0.2 and another at 0.7, can be identified. The isotherms can be therefore divided into three zones. The first zone ($a_w < 0.2$) represents the monolayer water; in the second zone, the adsorption/desorption occurs in the multilayer between 0.2 and 0.65, whereas water absorbed at $a_w > 0.65$ corresponds to water condensation in the film's pores followed by material dissolution (capillary water) (Miele et al., 2022). As shown in Fig. 4a, pure PBS film showed low water absorption ($0.57 \text{ g}_{\text{water}} \text{ g}_{\text{dry film}}^{-1}$ % at 0.9 a_w) as a result of its hydrophobic properties. The water absorption significantly increased with HBP inclusion and also depended on their size. The hydrophilic properties of natural fibers likely contribute to the composites' water uptake (Zhao et al., 2012). At 0.9 a_w , PBS/HBP-S displayed the highest water absorbed ($3.7 \text{ g}_{\text{water}} \text{ g}_{\text{dry film}}^{-1}$ %) compared to PBS/HBP-M and PBS/HBP-L which absorbed a similar amount of water, equal to 2.20 and $2.46 \text{ g}_{\text{water}} \text{ g}_{\text{dry film}}^{-1}$ %, respectively. The desorption isotherms for PBS and PBS/HBP composites films are shown in Fig. 4b. The isotherms of PBS/HBP composites film show hysteresis between the sorption and desorption branches in the a_w range roughly of 0.1-0.8. In this range the water content between the desorption and sorption isotherms differs more than 0.1%; the greatest differences occurred at a_w value of 0.7 and ranged between 0.2 and 0.5 $\text{g}_{\text{water}} \text{ g}_{\text{dry film}}^{-1}$ % for PBS/HBP-M and PBS/HBP-S, respectively. The experimental moisture adsorption data were well fitted to the GAB

model. HBP inclusion and fiber particle size significantly ($p < 0.05$) affected the GAB model parameters, which are listed in Table 6. The monolayer moisture content m_0 was the lowest in PBS film ($0.0022 \pm 0.001 \text{ g}_{\text{water}} \text{ g}_{\text{dry film}}^{-1}$), indicating a poor water binding capacity. PBS/HBP-S showed a higher m_0 value ($0.0083 \pm 0.000 \text{ g}_{\text{water}} \text{ g}_{\text{dry film}}^{-1}$) than PBS/HBP-M and PBS/HBP-L, for which no significant differences were observed (0.0063 ± 0.001 and $0.0065 \pm 0.002 \text{ g}_{\text{water}} \text{ g}_{\text{dry film}}^{-1}$). The findings imply that the incorporation of hop fiber may generate new water-binding sites, decreasing the hydrophobic nature of the matrix, especially in the presence of smaller HBP fibers. The strength of water binding in a monolayer is measured by the parameter C, or the sorption

Table 6

GAB model constants: m_0 , C and K values estimated by fitting moisture adsorption isotherms with the GAB model (Eq. 6) and R^2 of the model.

GAB constants	PBS	PBS/HBP-S	PBS/HBP-M	PBS/HBP-L
m_0 ($\text{g}_{\text{water}} \text{ g}_{\text{dry film}}^{-1}$)	0.0022 $\pm 0.001^a$	0.0083 $\pm 0.000^c$	0.0063 $\pm 0.001^b$	0.0065 $\pm 0.002^b$
C (-)	2.5345 $\pm 0.010^a$	7.3774 $\pm 0.011^c$	4.7777 $\pm 0.015^b$	4.4368 $\pm 0.010^b$
k (-)	0.7981 $\pm 0.005^a$	0.8541 $\pm 0.005^c$	0.8123 $\pm 0.008^b$	0.8351 $\pm 0.002^{bc}$
R^2	0.951 ± 0.001	0.998 ± 0.001	0.999 ± 0.001	0.999 ± 0.001

For each line, different letters correspond to significant differences among the samples ($p \leq 0.05$).

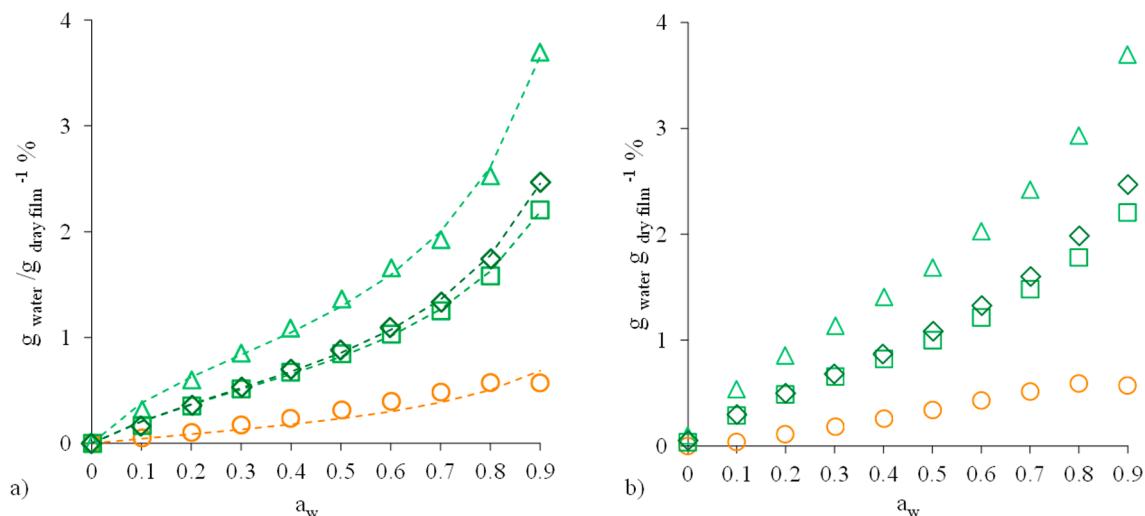


Fig. 4. Water adsorption/desorption isotherm of films. equilibrium moisture sorption (a) and desorption (b) isotherms (\circ PBS, Δ PBS/HBP-S, \square PBS/HBP-M, \diamond PBS/HBP-L). the dotted lines illustrate the GAB model fitting applied to the experimental sorption isotherm data.

energy constant. A higher C value indicates a stronger water-substrate contact in the monolayer and, as a result, a greater enthalpy difference between the monolayer and multilayer molecules (Cui et al., 2020; Fabra et al., 2010). For all films, K, which is a parameter related to the heat of multilayer sorption, falls between 0 and 1. The fact that the K value remains below 1 aligns with its physical interpretation; if K were greater than 1, it would suggest unlimited sorption, making the GAB model unsuitable (de Oliveira et al., 2017). Modifications of K caused by the presence of hop flour are linked to the interactions between the multilayer water and water present in its fully liquid state on the surface. The observed one-order-of-magnitude differences in C and K values are directly connected to the heat of sorption in both the monolayer and multilayer phases. These results are consistent with the chemical composition of the different hop fractions. PBS/HBP-S displayed the highest water absorption because the higher the cellulose content in hop fibres, the greater the amount of -OH groups available for water absorption. On the contrary, M and L hop fractions have a higher content of lignin which, being naturally hydrophobic, can limit water absorption, reducing the overall capacity of the film to retain moisture.

3.4. Antioxidant activity of PBS/HBP composites film

Fig. 5 illustrates the antioxidant activity of the films at the equilibrium time after contact with the ethanolic solution. Film prepared with total HBP showed the highest antioxidant activity with values of 4 ± 0.28 mg TEAC g_{film}^{-1} and 34.1 ± 1.04 mg TEAC g_{film}^{-1} for DPPH (Fig. 5a) and ABTS (Fig. 5b) assay, respectively. Considering film prepared with HBP fractions, the antioxidant activity varied between 3.5 ± 0.15 and 3.8 ± 0.28 mg TEAC g_{film}^{-1} for DPPH, and between 30.7 ± 1.41 and 33.7 ± 0.21 mg TEAC g_{film}^{-1} for ABTS. A mild effect of HBP fiber size on antioxidant activity was observed ($p=0.039$ for DPPH; $p=0.043$ for ABTS). However, antioxidant activity did not increase with HBP fiber size, as slightly higher values were observed for the film with particle size M than the other two.

A slight effect of HBP fiber size on the antioxidant activity of films in food simulants was also observed ($p=0.036$ for DPPH; $p=0.047$ for ABTS) (Fig. 6). The films prepared with medium-size HBP showed higher values than those prepared with the other sizes, confirming the results previously observed. The reduction of particle size can enhance the exposed surface area, thereby improving the availability of bioactive compounds (Aniško et al., 2024). However, this relationship is not linear: beyond a certain threshold, excessive fragmentation may

compromise compound stability or promote interactions that diminish their activity. For example, Idrovo Encalada et al. (2016) examined the effect of carrot fiber particle size (53, 105 and 210 μm) on composite films based on low-methoxyl pectin, including their antioxidant capacity. Films containing fibers with an intermediate particle size (105 μm) exhibited slightly higher antioxidant activity than those with smaller (53 μm) or larger (210 μm) particles, indicating a non-linear influence of particle size on antioxidant performance (Idrovo Encalada et al., 2016).

Contact time significantly affected antioxidant activity ($p < 0.05$). Considering the DPPH assay, antioxidant activity increased over time, reaching equilibrium after 7 days at values of 1.7 mg TEAC/g film. Considering the ABTS assay, antioxidant activity increased over time, reaching values around 23 mg TEAC/g film after 10 days. The rising activity observed over time indicates the progressive migration of antioxidant compounds from the film to the food simulants. No significant effect of food simulants on antioxidant activity measured with DPPH was observed. However, food simulants affected antioxidant activity measured with ABTS assay ($p < 0.05$) (Fig. 7). The greatest differences among samples were observed by ABTS assay using food simulants C and D1. These results suggested that simulants C and D1 had a higher capacity to solubilize and extract antioxidant compounds from the film. In comparison, simulants A and B had a slower and lower extraction capacity than C and D1. The antioxidant and radical-scavenging properties of hop biomass largely derive from its key bioactive constituents, including α -acids, β -acids, xanthohumol, and diverse phenolic compounds (Kontek et al., 2021; Chiancone et al., 2023). These compounds differ markedly in polarity and solubility, which critically shape their release behavior in food simulants. In particular, α -acids, β -acids, and xanthohumol, being predominantly hydrophobic, are more efficiently extracted when the films are in contact with simulants C and D1, whereas the more hydrophilic phenolic compounds show greater affinity for aqueous simulants (Paniagua-García et al., 2024).

Since simulants C and D1 solubilize antioxidants well, these films could be suitable for foods with a high-fat content or with an alcohol fraction, where the risk of oxidation is high, for which a more efficient release could help to preserve the flavor and quality of the product. They could also be suitable for aqueous or acidic foods, where the release, although lower, will be slower, i.e. where gradual and prolonged antioxidant protection is preferable.

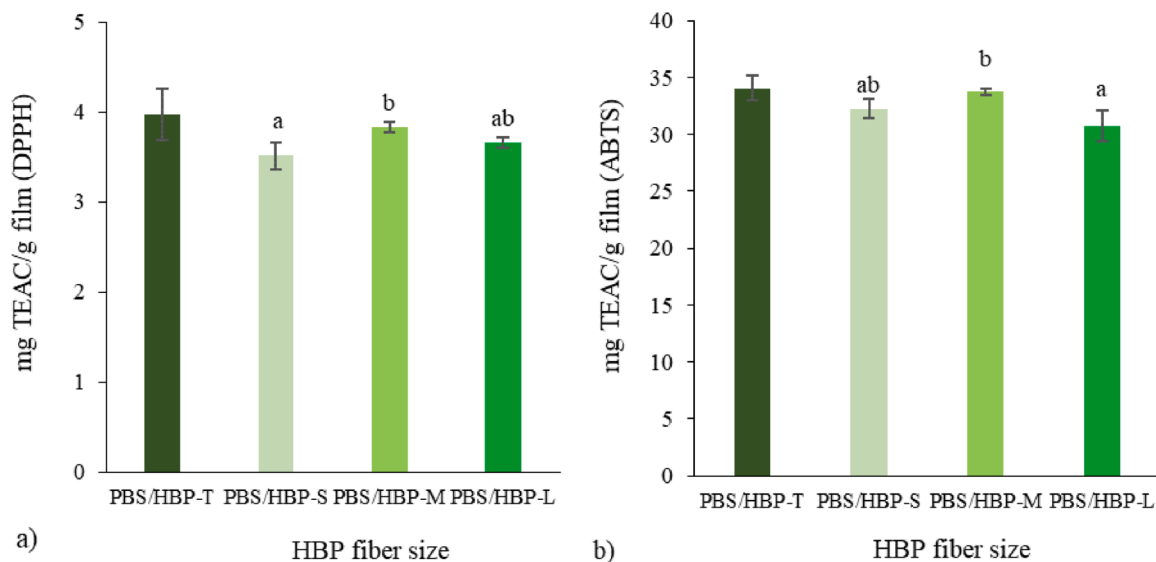


Fig. 5. Antioxidant activity of films in ethanolic solution. antioxidant activity of PBS/HBP composites film after contact with ethanolic solution measured by DPPH (a) and ABTS (b) assays. different letters indicate significant differences among the samples based on HBP fiber size ($p \leq 0.05$).

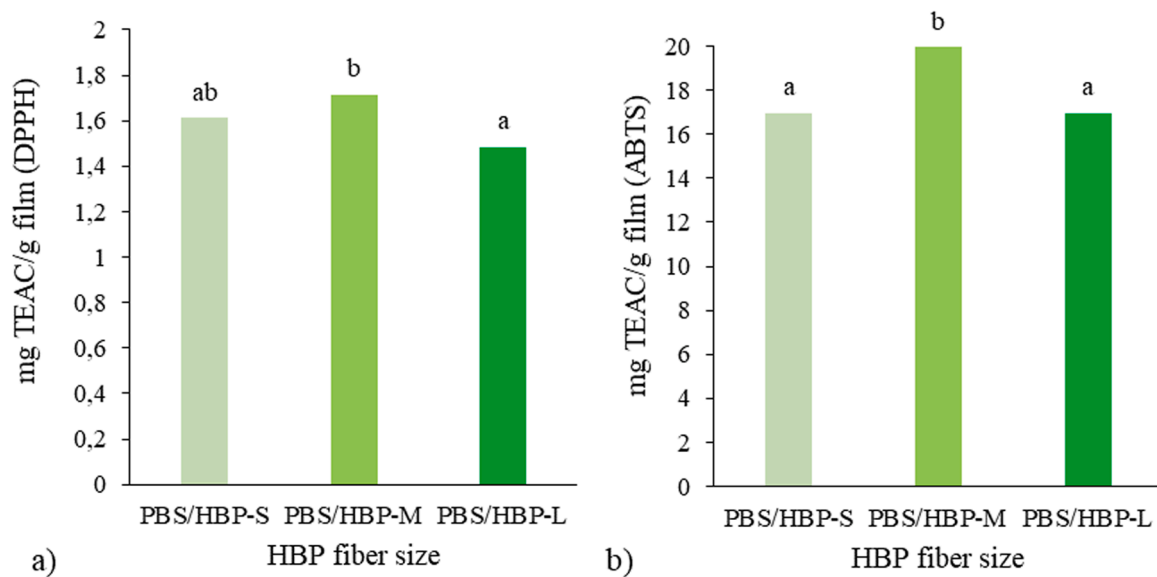


Fig. 6. Antioxidant activity PBS/HBP composites film in food simulants. antioxidant activity of PBS/HBP composites film prepared with different HBP fiber sizes after contact with food simulant measured by DPPH (a) and ABTS (b) assays. different letters indicate significant differences among the samples based on HBP fiber size ($p \leq 0.05$).

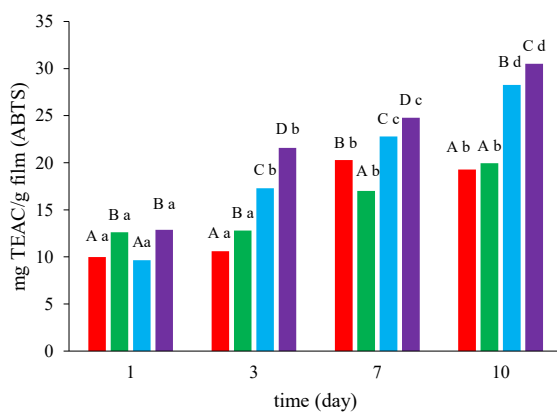


Fig. 7. Effect of food simulants on antioxidant activity. antioxidant activity of PBS/HBP composites film after contact with food simulant A (red color) B (green color) C (blue color) and D1 (purple color) after 1, 3, 7 and 10 days by ABTS assay. different lowercase letters indicate significant differences among the samples based on contact time ($p \leq 0.05$). Different uppercase letters denote significant differences among the samples based on the type of food simulant ($p \leq 0.05$).

4. Conclusions

This study demonstrates the successful valorization of hop by-product powder (HBP), either as a whole or fractionated into different particle sizes, as a functional additive for the development of biodegradable active packaging based on polybutylene succinate (PBS). Compared to previous studies focusing mainly on isolated plant parts, our findings reveal that the full hop biomass, traditionally considered agricultural waste, can provide significant functional benefits. The HBP fractions exhibited variations in hemicellulose, lignin, and cellulose content. Smaller fibers contained higher cellulose levels and demonstrated increased total (poly)phenol content and antioxidant activity. Adding HBP enhanced the elastic modulus and water absorption capacity of PBS films, while also making them darker and opaquer. However, fiber size had no significant effect on the mechanical and thermal properties of the films or their antioxidant capacity, suggesting that the fractionation process could be skipped, leading to significant

time savings. HBP retained its antioxidant activity when embedded in PBS and exhibited an effective release profile in food simulants. These films are particularly suitable for fatty food applications due to the higher solubilization of antioxidants in lipophilic simulants, yet they could also be effective for aqueous foods when a slower, more controlled release is required. Overall, these findings indicate that HBP can be successfully utilized to develop PBS films with enhanced functional properties, suggesting their effectiveness in food packaging. However, several limitations remain, including the lack of assessment of long-term stability, potential migration of non-target compounds, and performance under real-world storage conditions. Future work should address these aspects, along with scale-up feasibility and regulatory compliance, to advance HBP-based PBS films toward commercial application, bridging research and practical development of next-generation biodegradable active packaging.

Ethical statement

The enclosed paper, entitled Valorization of hops by-product for development of active poly(butylene succinate) film did not involve any studies with human participants or animals performed by any of the authors.

CRedit authorship contribution statement

Angela Borriello: Writing – review & editing, Writing – original draft, Visualization, Methodology, Investigation, Formal analysis. **Angela Marotta:** Writing – review & editing, Writing – original draft, Visualization, Methodology, Investigation, Formal analysis. **Leandra Leto:** Writing – review & editing, Writing – original draft, Methodology, Investigation, Formal analysis. **Martina Cirilini:** Writing – review & editing, Supervision. **Benedetta Chiancone:** Writing – review & editing, Supervision, Funding acquisition, Conceptualization. **Prospero Di Piero:** Writing – review & editing, Validation, Formal analysis. **Veronica Ambrogio:** Writing – review & editing, Supervision, Funding acquisition, Conceptualization. **Elena Torrieri:** Writing – review & editing, Supervision, Funding acquisition, Conceptualization.

Declaration of competing interest

The authors declare that they have no known competing financial interests or personal relationships that could have appeared to influence the work reported in this paper.

Acknowledgments

The authors would like to thank Packtin s.r.l. who kindly provided the hop vegetative biomass powder.

This study was carried out within 1) the Agritech National Research Center (Task 8.1.3. Valorization of the waste to obtain biomaterials) and received funding from the European Union via Next-Generation EU (PIANO NAZIONALE DI RIPRESA E RESILIENZA (PNRR)—MISSIONE 4 COMPONENTE 2, INVESTIMENTO 1.4—D.D. 1032 17/06/2022022, CN00000022); 2) University of Parma through the action “Bando di Ateneo 2021 per la ricerca” co-funded by MUR—Italian Ministry of Universities and Research—D.M. 737/2021—PNR—PNRR—NextGenerationEU; Project Title: HOPLURE—Hop leaves, an unexplored resource. This manuscript reflects only the authors' views and opinions, and neither the European Union nor the European Commission can be considered responsible for them.

Supplementary materials

Supplementary material associated with this article can be found, in the online version, at [doi:10.1016/j.fufo.2026.100899](https://doi.org/10.1016/j.fufo.2026.100899).

Data availability

Data will be made available on request.

References

- Abram, V., Čeh, B., Vidmar, M., Hercezi, M., Lazić, N., Bucik, V., Smole Možina, S., Košir, I.J., Kač, M., Demšar, L., Ulrih, N.P., 2025. A comparison of antioxidant and antimicrobial activity between hop leaves and hop cones. *Ind. Crops Prod.* 64, 124–134. <https://doi.org/10.1016/j.indcrop.2014.11.008>.
- Aniško, J., Kosmela, P., Cichočka, J., Andrzejewski, J., Barczewski, M., 2024. How the dimensions of plant filler particles affect the oxidation-resistant characteristics of polyethylene-based composite materials. *Materials* 17, 4825. <https://doi.org/10.3390/ma17194825>.
- Ayeni, A.O., Adeeyo, O.A., Oressegun, O.M., Oladimeji, T.E., 2015. Compositional analysis of lignocellulosic materials: evaluation of an economically viable method suitable for woody and non-woody biomass. *Am. J. Eng. Res.* 4, 14–19.
- Aziman, N., Kian, L.K., Jawaid, M., Sanny, M., Alamery, S., 2021. Morphological, structural, thermal, permeability, and antimicrobial activity of PBS and PBS/TPS films incorporated with biomaster-silver for food packaging application. *Polymer* 13, 391. <https://doi.org/10.3390/polym13030391>.
- Barczewski, M., Aniško, J., Hejna, A., Mysiukiewicz, O., Kosmela, P., Salasińska, K., Boczkowska, A., Przybylska-Balcerek, A., Stuper-Szablewska, K., 2023. Ground lemon and stevia leaves as renewable functional fillers with antioxidant activity for high-density polyethylene composites. *Clean Technol. Environ. Policy* 25, 3345–3361. <https://doi.org/10.1007/s10098-023-02565-5>.
- Bhargava, N., Sharanagat, V.S., Mor, R.S., Kumar, K., 2020. Active and intelligent biodegradable packaging films using food and food waste-derived bioactive compounds: a review. *Trends Food Sci. Technol.* 105, 385–401. <https://doi.org/10.1016/j.tifs.2020.09.015>.
- Borriello, A., Miele, N.A., Volpe, S., Basile, G., Verrillo, M., Spaccini, R., Cavella, S., Romano, R., Torrieri, E., 2025. Valorization of spent coffee ground through the development of alginate-based composite antioxidant films: Physicochemical properties and release kinetics. *Appl. Food Res.* 5, 100778. <https://doi.org/10.1016/j.jafres.2025.100778>.
- Carbone, K., Macchioni, V., Petrella, G., Cicero, D.O., 2020. Exploring the potential of microwaves and ultrasounds in the green extraction of bioactive compounds from *Humulus lupulus* for the food and pharmaceutical industry. *Ind. Crops Prod.* 156, 112888. <https://doi.org/10.1016/j.indcrop.2020.112888>.
- Censi, R., Vargas Peregrina, D., Gigliobianco, M.R., Lupidi, G., Angeloni, C., Pruccoli, L., Tarozzi, A., Di Martino, P., 2021. New antioxidant ingredients from brewery by-products for cosmetic formulations. *Cosmetics* 8, 96. <https://doi.org/10.3390/cosmetics8040096>.
- Chiancone, B., Guarrasi, V., Leto, L., Del Vecchio, L., Calani, L., Ganino, T., Galaverni, M., Cirilini, M., 2023. Vitro-derived hop (*Humulus lupulus* L.) leaves and roots as source of bioactive compounds: antioxidant activity and polyphenolic profile. *Plant Cell Tissue Organ Cult.* 153, 295–306. <https://doi.org/10.1007/s11240-023-02462-1>.
- Cui, Y., Gao, S., Zhang, R., Cheng, L., Yu, J., 2020. Study on the moisture absorption and thermal properties of hygroscopic exothermic fibers and related interactions with water molecules. *Polymer* 12, 98. <https://doi.org/10.3390/polym12010098>.
- De'Nobili, M.D., Bernhardt, D.C., Basanta, M.F., Rojas, A.M., 2021. Sunflower (*Helianthus annuus* L.) seed hull waste: Composition, antioxidant activity, and filler performance in pectin-based film composites. *Front. Nutr.* 8, 777214. <https://doi.org/10.3389/fnut.2021.777214>.
- de Oliveira, G.H.H., Corrêa, P.C., de Oliveira, A.P.L.R., dos Reis, R.C., Devilla, I.A., 2017. Application of GAB model for water desorption isotherms and thermodynamic analysis of sugar beet seeds. *J. Food Process Eng.* 40, e12278. <https://doi.org/10.1111/jfpe.12278>.
- Duguma, H.T., Khule, P., McArdle, A., Fennell, K., Almenar, E., 2023. Turning agricultural waste into packages for food: A literature review from origin to end-of-life. *Food Packag. Shelf Life* 40, 101166. <https://doi.org/10.1016/j.fpsl.2023.101166>.
- Durling, N.E., Catchpole, O.J., Grey, J.B., Webby, R.F., Mitchell, K.A., Foo, L.Y., Perry, N.B., 2007. Extraction of phenolics and essential oil from dried sage (*Salvia officinalis*) using ethanol–water mixtures. *Food Chem.* 101, 1417–1424. <https://doi.org/10.1016/j.foodchem.2006.03.050>.
- Fabra, M.J., Talens, P., Chiralt, A., 2010. Water sorption isotherms and phase transitions of sodium caseinate–lipid films as affected by lipid interactions. *Food Hydrocoll.* 24, 384–391. <https://doi.org/10.1016/j.foodhyd.2009.11.004>.
- Antony, A., Farid, M., 2022. Effect of temperatures on polyphenols during extraction. *Appl. Sci.* 12 (4), 2107. <https://doi.org/10.3390/app12042107>.
- Hanani, Z.N., Yee, F.C., Nor-Khaizura, M.A.R., 2019. Effect of pomegranate (*Punica granatum* L.) peel powder on the antioxidant and antimicrobial properties of fish gelatin films as active packaging. *Food Hydrocoll.* 89, 253–259. <https://doi.org/10.1016/j.foodhyd.2018.10.007>.
- Harder, N., Rodriguez-Urbe, A., Snowdon, M.R., Misra, M., Mohanty, A.K., 2023. Hop natural fiber-reinforced poly (butylene succinate-co-butylene adipate) (PBSA) biodegradable plastics: effect of fiber length on the performance of biocomposites. *Mater. Adv.* 4, 1502–1514. <https://doi.org/10.1039/D2MA000831A>.
- Hejna, A., Barczewski, M., Kosmela, P., Aniško, J., Szulc, J., Skórczewska, K., Piasecki, A., Kuang, T., 2024. More than just a beer—Brewers' spent grain, spent hops, and spent yeast as potential functional fillers for polymer composites. *Waste Manag.* 180, 23–35. <https://doi.org/10.1016/j.wasman.2024.03.023>.
- Idrovo Encalada, A.M., Basanta, M.F., Fissore, E.N., De'Nobili, M.D., Rojas, A.M., 2016. Carrot fiber (CF) composite films for antioxidant preservation: Particle size effect. *Carbohydr. Polym.* 136, 1041–1051. <https://doi.org/10.1016/j.carbpol.2015.09.109>.
- Jimenez-Lopez, C., Fraga-Corral, M., Carpena, M., García-Oliveira, P., Echave, J., Pereira, A.G., Laureço-Lopes, C., Prieto, M.A., Simal-Gandara, J., 2020. Agriculture waste valorisation as a source of antioxidant phenolic compounds within a circular and sustainable bioeconomy. *Food Funct.* 11, 4853–4877. <https://doi.org/10.1039/D0FO00937G>.
- Khan, R.M., Volpe, S., Sadiq, M.B., Giannino, F., Torrieri, E., 2022. Correlating in silico elucidation of interactions between hydroxybenzoic acids and casein with in vitro release kinetics for designing food packaging. *Food Packag. Shelf Life.* 32, 100859. <https://doi.org/10.1016/j.fpsl.2022.100859>.
- Kontek, B., Jedrejek, D., Oleszek, W., Olas, B., 2021. Antiradical and antioxidant activity in vitro of hops-derived extracts rich in bitter acids and xanthohumol. *Ind. Crops Prod.* 161, 113208. <https://doi.org/10.1016/j.indcrop.2020.113208>.
- Leto, L., Favari, C., Agosti, A., Del Vecchio, L., Di Fazio, A., Bresciani, L., Mena, P., Guarrasi, V., Cirilini, M., Chiancone, B., 2024. Evaluation of in vitro-derived hop plantlets, cv. columbus and magnum, as potential source of bioactive compounds. *Antioxidants* 13, 909. <https://doi.org/10.3390/antiox13080909>.
- Li, Y., Sang, L., Wei, Z., Ding, C., Chang, Y., Chen, G., Zhang, W., Liang, J., 2015. Mechanical properties and crystallization behavior of poly (butylene succinate) composites reinforced with basalt fiber. *J. Therm. Anal. Calorim.* 122, 261–270. <https://doi.org/10.1007/s10973-015-4732-8>.
- Łopusiewicz, E., Zdanowicz, M., Macieja, S., Kowalczyk, K., Bartkowiak, A., 2021. Development and characterization of bioactive poly(butylene-succinate) films modified with quercetin for food packaging applications. *Polymers* 13 (11), 1798. <https://doi.org/10.3390/polym13111798>.
- Macchioni, V., Picchi, V., Carbone, K., 2022. Hop leaves as an alternative source of health-active compounds: effect of genotype and drying conditions. *Plants* 11, 99. <https://doi.org/10.3390/plants11010099>.
- Macieja, S., Bartkowiak, A., Mizielińska, M., 2025. Preparation and characterization of poly(butylene succinate) films modified with sea buckthorn (*hippophae rhamnoides* L.) extract for packaging applications. *Appl. Sci.* 15 (4), 2099. <https://doi.org/10.3390/app15042099>.
- Makri, S.P., Xanthopoulou, E., Klonos, P.A., Grigoropoulos, A., Kyritsis, A., Tsachouridis, K., Anastasiou, A., Deligkiozi, I., Nikolaidis, N., Bikiaris, D.N., 2022. Effect of micro- and nano-lignin on the thermal, mechanical, and antioxidant properties of biobased PLA–lignin composite films. *Polymer* 14, 5274. <https://doi.org/10.3390/polym14235274>.
- Marotta, A., Borriello, A., Khan, M.R., Cavella, S., Ambrogi, V., Torrieri, E., 2025. Boosting Food Packaging Sustainability Through the Valorization of Agri-Food Waste and By-Products. *Polym.* 17, 735. <https://doi.org/10.3390/polym17060735>.
- Martelli, F., Favari, C., Mena, P., Guazzetti, S., Ricci, A., Del Rio, D., Lazzi, C., Neviani, E., Bernini, V., 2020. Antimicrobial and fermentation potential of *Himanthalia elongata* in food applications. *Microorg.* 8, 248. <https://doi.org/10.3390/microorganisms8020248>.
- Miele, N.A., Volpe, S., Torrieri, E., Cavella, S., 2022. Improving physical properties of sodium caseinate based coating with the optimal formulation: Effect on strawberries'

- respiration and transpiration rates. *J. Food Eng.* 331, 111123. <https://doi.org/10.1016/j.foodeng.2022.111123>.
- Mizielnińska, M., Zdanowicz, M., Tarnowiecka-Kuca, A., Bartkowiak, A., 2024. The Influence of functional composite coatings on the properties of polyester films before and after accelerated UV aging. *Materials* 17 (13), 3048. <https://doi.org/10.3390/ma17133048>.
- Mirowski, J., Oliwa, R., Oleksy, M., Rój, E., Tomaszewska, J., Mizera, K., Ryszkowska, J., 2021. Composites of Poly (vinyl chloride) with Residual Hops after Supercritical Extraction in CO₂. *Polym* 13, 2736. <https://doi.org/10.3390/polym13162736>.
- Mohamad, N., Mazlan, M.M., Tawakkal, I.S.M.A., Talib, R.A., Kian, L.K., Jawaid, M., 2022. Characterization of active polybutylene succinate films filled essential oils for food packaging application. *J. Polym. Environ.* 30, 585–596. <https://doi.org/10.1007/s10924-021-02198-z>.
- Mohd Basri, M.S., Abdul Karim Shah, N.N., Sulaiman, A., Mohamed Amin Tawakkal, I.S., Mohd Nor, M.Z., Ariffin, S.H., Abdul Ghani, N.H., Mohd Salleh, F.S., 2021. Progress in the Valorization of Fruit and Vegetable Wastes: Active Packaging, Biocomposites, By-Products, and Innovative Technologies Used for Bioactive Compound Extraction. *Polym.* 13, 3503. <https://doi.org/10.3390/polym13203503>.
- Netshiluvhi, T.R., Eloff, J.N., 2024. Temperature and water stresses on antioxidant activity of selected medicinal plants have implications for sustainable use and global warming. *S. Afr. J. Bot.* 170, 177–180. <https://doi.org/10.1016/j.sajb.2024.05.028>.
- Ning, P., Yang, G., Hu, L., Sun, J., Shi, L., Zhou, Y., Wang, Z., Yang, J., 2021. Recent advances in the valorization of plant biomass. *Biotechnol. Biofuels* 14, 102. <https://doi.org/10.1186/s13068-021-01949-3>.
- Nuamduang, P., Auras, R., Winotapun, C., Hararak, B., Wanmolee, W., Leelaphiwat, P., 2024. Enhanced antifungal properties of poly (butylene succinate) film with lignin nanoparticles and trans-cinnamaldehyde for mango packaging. *Int. J. Biol. Macromol.* 267, 131185. <https://doi.org/10.1016/j.ijbiomac.2024.131185>.
- Ortega, F., Versino, F., López, O.V., García, M.A., 2022. Biobased composites from agro-industrial wastes and by-products. *Emerg. Mater.* 5, 873–921. <https://doi.org/10.1007/s42247-021-00319-x>.
- Ou-Yang, Q., Guo, B., Xu, J., 2018. Preparation and characterization of poly (butylene succinate)/polylactide blends for fused deposition modeling 3D printing. *ACS Omega* 3, 14309–14317. <https://doi.org/10.1021/acsomega.8b02549>.
- Paniagua-García, A.I., Ruano-Rosa, D., Díez-Antolínez, R., 2024. Fractionation of high-value compounds from hops using an optimised sequential extraction procedure. *Antioxidants* 13 (1), 45. <https://doi.org/10.3390/antiox13010045>.
- Panzella, L., Moccia, F., Nasti, R., Marzorati, S., Verotta, L., Napolitano, A., 2020. Bioactive phenolic compounds from agri-food wastes: an update on green and sustainable extraction methodologies. *Front. Nutr.* 7, 60. <https://doi.org/10.3389/fnut.2020.00060>.
- Pattaraudomchok, P., Winotapun, C., Tameesrisuk, M., Hararak, B., 2024. Essential oils loaded biodegradable PBAT/PBS films as young coconut packaging after harvest. *Food Packag. Shelf Life* 44, 101322. <https://doi.org/10.1016/j.fpsl.2024.101322>.
- Pothinuch, P., Promsorn, J., Sablani, S.S., Harnkarnsujarit, N., 2024. Antioxidant release, morphology and packaging properties of gallic acid incorporated biodegradable PBAT blended PBS active packaging. *Food Packag. Shelf Life*. 43, 101304.
- Qin, S., Li, Z., Ren, Z., Miao, Y., Zhang, Z., Xie, Y., Liu, S., Wang, Q., Pittman, C.U., 2025. Polybutylene succinate/lignin composites with tunable optical, mechanical, and thermal properties based on fractionation treatment. *Int. J. Biol. Macromol.* 298, 139603. <https://doi.org/10.1016/j.ijbiomac.2025.139603>.
- Rodolfi, M., Chiancone, B., Liberatore, C.M., Fabbri, A., Cirlini, M., Ganino, T., 2019. Changes in chemical profile of Cascade hop cones according to the growing area. *J. Sci. Food Agric.* 99, 6011–6019. <https://doi.org/10.1002/jsfa.9876>.
- Rodriguez-Urbe, A., Harder, N., Misra, M., Mohanty, A.K., 2023. Biocomposites from poly (butylene succinate-co-butylene adipate) biodegradable plastic and hop natural fiber: studies on the effect of compatibilizer on performance of the composites. *Compos. C Open Access*. 12, 100408. <https://doi.org/10.1016/j.jcom.2023.100408>.
- Sabbatini, G., Mari, E., Ortore, M.G., Di Gregorio, A., Fattorini, D., Di Carlo, M., Galeazzi, R., Vignaroli, C., Simoni, S., Giorgini, G., Guarrasi, V., Chiancone, B., Leto, L., Cirlini, M., Del Vecchio, L., Mangione, M.R., Vilasi, S., Minnelli, C., Mobbili, G., 2024. Hop leaves: from waste to a valuable source of bioactive compounds – a multidisciplinary approach to investigating potential applications. *Heliyon* 10, e37593. <https://doi.org/10.1016/j.heliyon.2024.e37593>.
- Santagostini, L., Caporali, E., Giuliani, C., Bottoni, M., Ascrizzi, R., Araneo, S.R., Papini, A., Flamini, G., Fico, G., 2020. *Humulus lupulus L.* cv. Cascade grown in Northern Italy: morphological and phytochemical characterization. *Plant Biosyst.* 154, 316–325. <https://doi.org/10.1080/11263504.2019.1610111>.
- Santarelli, V., Neri, L., Carbone, K., Macchioni, V., Pittia, P., 2022. Use of conventional and innovative technologies for the production of food grade hop extracts. *Focus Bioact. Compd. Antioxid. Act. Plants* 11, 41. <https://doi.org/10.3390/plants11010041>.
- Santos, L.G., Gomes, B.M., da Silva Noda, K., Martins, V.G., 2025. Trub brewery waste as a novel and sustainable protein source for the development of active packaging materials. *Int. J. Biol. Macromol.* 313, 144328. <https://doi.org/10.1016/j.ijbiomac.2025.144328>.
- Sarraf, C., Desjardins, Y., Leonhart, S., Gosselin, A., Gosselin, G., 2012. Agronomic and nutraceutical potential of hops (*Humulus Lupulus L.*) grown in Quebec. Canada. *Acta Hort.* 1010, 155–161. <https://doi.org/10.17660/ActaHortic.2013.1010.18>.
- Versino, F., García, M.A., 2018. Particle size distribution effect on cassava starch and cassava bagasse biocomposites. *ACS Sustain. Chem. Eng.* 7, 1052–1060. <https://doi.org/10.1021/acssuschemeng.8b04700>.
- Viola, E., Leto, L., Piazzese, D., Indelicato, S., Bongiorno, D., Lino, C., Garofalo, G., Bigi, F., Agosti, A., Guarrasi, V., Indovino, E., Botta, L., Cirlini, M., Gaglio, R., Barbera, M., Settanni, L., Chiancone, B., 2025. Exploring lactic acid bacteria diversity of hop plant by-products to develop a multi-strain starter culture to be used in hop-supplemented sourdough bread. *Food Res. Int.* 219, 117007. <https://doi.org/10.1016/j.foodres.2025.117007>.
- Wongphan, P., Nampanya, P., Chakpha, W., Promhuad, K., Laorenza, Y., Leelaphiwat, P., Bumbudsanpharoke, N., Sodsai, J., Lorenzo, J.M., Harnkarnsujarit, N., 2023. Lesser galangal (*Alpinia officinarum Hance*) essential oil incorporated biodegradable PLA/PBS films as shelf-life extension packaging of cooked rice. *Food Packag. Shelf Life*. 37, 101077. <https://doi.org/10.1016/j.fpsl.2023.101077>.
- Xu, Y., Liu, C., Qiao, L., Zhu, K., Tan, H., Dong, S., Lin, Z., 2022. Crystallization and dynamic mechanical behavior of coir fiber reinforced poly (butylene succinate) biocomposites. *J. Renew. Mater.* 10, 1039. <https://doi.org/10.32604/jrm.2022.017239>.
- Yang, C., Tang, H., Wang, Y., Liu, Y., Wang, J., Shi, W., Li, L., 2019. Development of PLA-PBSA based biodegradable active film and its application to salmon slices. *Food Packag. Shelf Life*. 22, 100393. <https://doi.org/10.1016/j.fpsl.2019.100393>.
- Yeasmen, N., Orsat, V., 2023. Phenolic mapping and associated antioxidant activities through the annual growth cycle of sugar maple leaves. *Food Chem.* 428, 136882. <https://doi.org/10.1016/j.foodchem.2023.136882>.
- Zafar, M.F., Siddiqui, M.A., 2021. Effect of filler loading and size on the mechanical and morphological behaviour of natural fibre-reinforced polystyrene composites. *Adv. Mater. Process. Technol.* 7, 647–659. <https://doi.org/10.1080/2374068X.2020.1793261>.
- Zhang, Y., Li, Z., Zeng, J., Gao, H., Qi, J., 2025. Barrier properties characterization and release kinetics study of citrus fibers-reinforced functional starch composites. *Food Hydrocoll* 164, 111195. <https://doi.org/10.1016/j.foodhyd.2025.111195>.
- Zhao, Y., Qiu, J., Feng, H., Zhang, M., 2012. The interfacial modification of rice straw fiber reinforced poly(butylene succinate) composites: Effect of aminosilane with different alkoxy groups. *J. Appl. Polym. Sci.* 125, 3211–3220. <https://doi.org/10.1002/app.36502>.
- Zou, Y., Reddy, N., Yang, Y., 2010. Using hop bines as reinforcements for lightweight polypropylene composites. *J. Appl. Polym. Sci.* 116, 2366–2373. <https://doi.org/10.1002/app.31770>.